Metamorphic Evolution of Garnet-bearing Epidote-Barroisite Schist from the Meratus Complex in South Kalimantan, Indonesia

Nugroho Imam Setiawan[1], Yasuhito Osanai[2], Nobuhiko Nakano[2], Tatsuro Adachi[2], and Amril Asy'ari[3]

[1]Geological Engineering Department, Faculty of Engineering, Universitas Gadjah Mada, Yogyakarta, Indonesia
[2]Division of Earth Sciences, Faculty of Social and Cultural Studies, Kyushu University, Fukuoka, Japan
[3]Mining Department, Banjarmasin State Polytechnic, Banjarmasin, Indonesia

Corresponding author: nugroho.setiawan@ugm.ac.id
Manuscript received: January 6, 2015; revised: March 4, 2015;
approved: August 26, 2015; available online: October 23, 2015

Abstract - This paper presents metamorphic evolution of metamorphic rocks from the Meratus Complex in South Kalimantan, Indonesia. Eight varieties of metamorphic rocks samples from this location, which are garnet-bearing epidote-barroisite schist, epidote-barroisite schist, glaucophane-quartz schist, garnet-muscovite schist, actinolite-talc schist, epidote schist, muscovite schist, and serpentinite, were investigated in detail its petrological and mineralogical characteristics by using polarization microscope and electron probe micro analyzer (EPMA). Furthermore, the pressure-temperature path of garnet-bearing epidote-barroisite schist was estimated by using mineral parageneses, reaction textures, and mineral chemistries to assess the metamorphic history. The primary stage of this rock might be represented by the assemblage of glaucophane + epidote + titanite ± paragonite. The assemblage yields 1.7 - 1.0 GPa in assumed temperature of 300 - 550 °C, which is interpreted as maximum pressure limit of prograde stage. The peak P-T condition estimated on the basis of the equilibrium of garnet rim, barroisite, phengite, epidote, and quartz, yields 547 - 690 °C and 1.1 - 1.5 GPa on the albite epidote amphibolite-facies that correspond to the depth of 38 - 50 km. The retrograde stage was presented by changing mineral compositions of amphiboles from the Si-rich barroisite to the actinolite, which lies near 0.5 GPa at 350 °C. It could be concluded that metamorphic rocks from the Meratus Complex experienced low-temperature and high-pressure conditions (blueschist-facies) prior to the peak metamorphism of the epidote amphibolite-facies. The subduction environments in Meratus Complex during Cretaceous should be responsible for this metamorphic condition.

Keywords: garnet-bearing epidote-barroisite schist, pressure-temperature path, high-pressure metamorphic rocks, Meratus Complex, South Kalimantan

INTRODUCTION

Background

The Meratus Complex lies in the South Kalimantan extending in trend of NE-SW (Figure 1). The metamorphic rocks cropping out in this location have been considered as part of Cretaceous subduction fossils in central Indonesia, which widely spread throughout Central Java, South Sulawesi, and South Kalimantan (Miyazaki *et al.*, 1996; 1998; Parkinson *et al.*, 1998; Kadarusman *et al.*, 2007). The studies of the high-pressure metamorphic rocks, especially their prograde and retrograde pressure-temperature paths, provide important constraint on the tectonic processes of ancient subduction zone in the central Indonesia.
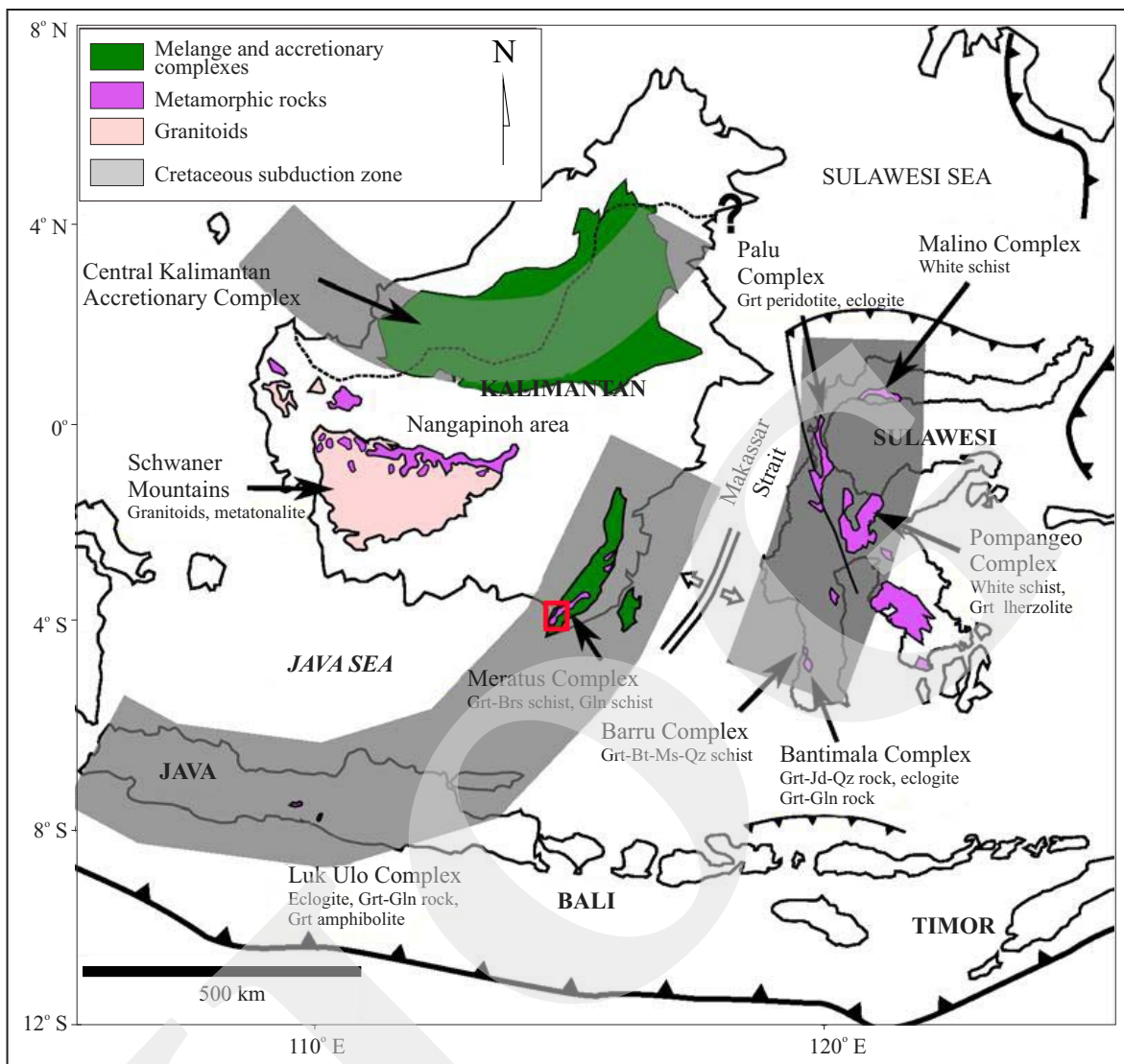
Figure 1. General types of metamorphic rocks in central Indonesia region. The study area is in the Meratus Complex of South Kalimantan. Metamorphic rock information database of the Schwaner Mountains from Williams *et al.* (1988), and Setiawan *et al.* (2013). The Luk Ulo Complex from Wakita *et al.* (1994b), Miyazaki *et al.* (1998), Asikin *et al.* (2007), and Kadarusman *et al.* (2007). The Meratus Complex from Parkinson *et al.* (1998), Sikumbang and Heryanto (2009), and Setiawan (2013). Barru Complex from Setiawan (2013). The Bantimala Complex from Sukamto (1982), Wakita *et al.* (1994a, 1996, 1998), Miyazaki *et al.* (1996), Parkinson *et al.* (1998), and Setiawan (2013). The Palu Complex from Kadarusman and Parkinson (2000), and Kadarusman *et al.* (2004). The Malino Complex from Leeuwen *et al.* (2006). The Pompangeo Complex from Parkinson (1998). Grt = garnet; Qz = quartz; Brs = Barroisite; Ms = muscovite; Gln = glaucophane.

Zulkarnain (2003) reported the occurences of quartz-chloritoid rocks from this location and concluded it was derived from pelitic schist in an accretionary complex environment. Moreover, Sikumbang and Heryanto (2009) reported occurences of several metamorphic rocks from this location. One of them is barroisite-epidote schist. Parkinson *et al.* (1998) described the occurrence of glaucophane- and kyanite-bearing quartz schist in this location and also suggested that the presence of Mg-rich chloritoid implied recrystallization at pressure of ~1.8 GPa or higher, which recommended as a part of high-pressure metamorphic terranes in central Indonesia (Luk-Ulo Complex in Central Java, Bantimala Complex in South Sulawesi). However, detailed observations of P-T evolution, particularly on the reaction texture of prograde, peak, and retrograde

stages have not been reported. In this paper, we present a petrographic description and minerals chemistry analysis of representative samples of newly found garnet-bearing epidote- barroisite schist from the Meratus Complex, South Kalimantan (Figures 1 and 2), and discuss its P-T evolution. Mineral chemistries of representative samples were analyzed using JEOL JXA-8530F electron probe micro analyzer (EPMA) at Kyushu University, Japan. The analytical condition of EPMA was set an accelerating voltage of 15 kV, a probe current of 12 nA and a beam diameter

of 2 μm. Natural mineral samples (ASTIMEX-MINM-53) and synthesized oxide samples (P and H Block No. SP00076) were used as standards for the quantitative chemical analyses. Mineral abbreviation in this paper follows Whitney and Evans (2010).

Constraining the prograde peak and retrograde P-T path are very important for geodynamic interpretations in the region. Particularly in high-pressure metamorphic terranes, prograde to retrograde histories are relevant to the processes of deep subduction and subsequent exhumation. The
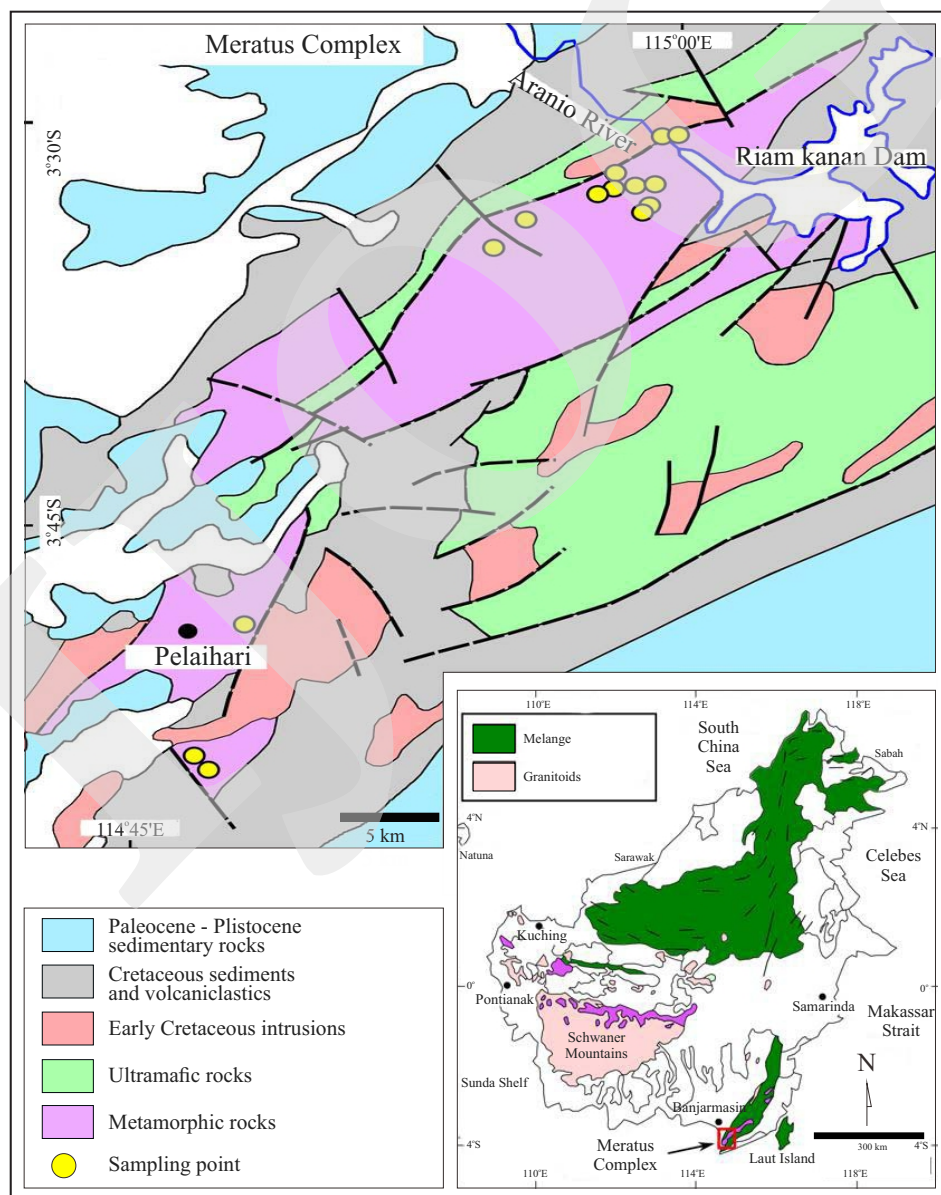

Figure 2. Simplified geological map and sample localities in the Meratus Complex, South Kalimantan (modified after Sikumbang and Heryanto, 2009). Insert map is location of the complex within the Kalimantan Island.

conclusion will address the metamorphic evolution of Meratus Complex and possible linkage with the other metamorphic terranes in central Indonesia. Furthermore, the authors also compare the results of the study with other high-pressure metamorphic terranes in central Indonesia (Bantimala Complex, South Sulawesi; Luk Ulo Complex, Central Java) for the sake of reconsidering the Mesozoic tectono-metamorphic development of the eastern margin of the Sundaland.

Geological Outline

The Cretaceous subduction complex, which is represented by the occurrence of accretionary unit including mélanges, pillow basalts, dismembered ophiolites, cherts, serpentinites, and garnet lherzolite are sporadically exposed in the central Indonesia region through the Java, Kalimantan, and Sulawesi Islands (Sukamto, 1982; Wakita *et al*., 1994a, 1994b, 1996, 1998; Miyazaki *et al*., 1996, 1998; Parkinson *et al*., 1998; Wilson and Moss, 1999; Kadarusman and Parkinson, 2000). The distribution of the accretionary units and metamorphic rocks are shown in Figure 1. Most of the metamorphic rocks exposing in the complexes occur in a limited areas and are bounded by the thrust fault with other units such as dismembered ophiolites, cherts, mélanges, and serpentinites (Sukamto, 1982; Asikin *et al*., 2007; Sikumbang and Heryanto, 2009).

In the Meratus and Bobaris Mountains of South Kalimantan, the metamorphic rocks crop out in the most southern part of the Meratus Mountains namely as the Meratus Complex. The Meratus Complex extends in the trend of NE–SW (Sikumbang and Heryanto, 2009; Figure 2). The metamorphic rocks occur as wedge-shaped tectonic blocks in fault contact with ultramafic rocks and Cretaceous sedimentary rocks (Parkinson *et al*., 1998). The dominant lithologies in this complex are serpentinized peridotite and pyroxenite, gabbro, plagiogranite intrusions, shale-matrix mélange with clasts of limestone, chert and basalt (Laut Island), pelagic sediments with a Middle Jurassic-late Early Cretaceous radiolarian biostratigraphy, clastic and carbonate sediments, and various low-grade schists (Wakita *et al*., 1998;

Parkinson *et al*., 1998; Sikumbang and Heryanto, 2009). These formations are unconformably overlain by Late Cretaceous turbidites and volcaniclastics (Figure 2). Cretaceous magmatic rocks of island-arc with calc-alkaline affinity intruded the Meratus Complex (Yuwono *et al*., 1988). The magmatic rocks are rhyolite, dacite, andesite, basalt, granite, diorite, and gabbro with the age ranges of 92 - 72 Ma (Yuwono *et al*., 1988).

Sikumbang and Heryanto (2009) reported metamorphic rocks of quartz-muscovite schist, quartzite, barroisite-epidote schist, and metagabbro. Parkinson *et al*. (1998) described the occurrence of glaucophane- and kyanite-bearing quartz schist in this location. They also suggested that the presence of Mg-rich chloritoid implied recrystallization at a pressure of ~1.8 GPa or higher. The K-Ar dating of various mica schists yielded ages ranging between 110 - 180 Ma, which are in the similar age with the metamorphic rocks in South Sulawesi and Central Java (Wakita *et al*., 1998; Sikumbang and Heryanto, 2009). Furthermore, Wakita *et al*. (1998) and Parkinson *et al*. (1998) suggested the occurrence of high-pressure metamorphic rocks in this location were products of a Cretaceous subduction beneath Sundaland.

RESULTS AND ANALYSES

Modes of Occurrences and Sample Descriptions

The blueschist- to amphibolite-facies rocks (*e.g.* epidote-barroisite schist discussed in this study) occur in the Aranio River (Figures 2 and 3a - c). The schist consists of garnet- and quartz-rich layers which has 80ºW trending foliation from north with dipping 66º to north (Figures 3b and c). In the southern part of the complex, only serpentinized peridotites were identified as metamorphic rocks and the others are ultramafic rocks and mafic rocks such as peridotite, olivine-gabbro, and hornblende-gabbro. The exposure of serpentinite could be found throughout in the complex (Figures 2 and 3d). Other types of metamorphic rocks are mainly tremolite-talc schist, muscovite schist, and epidote schist. However,
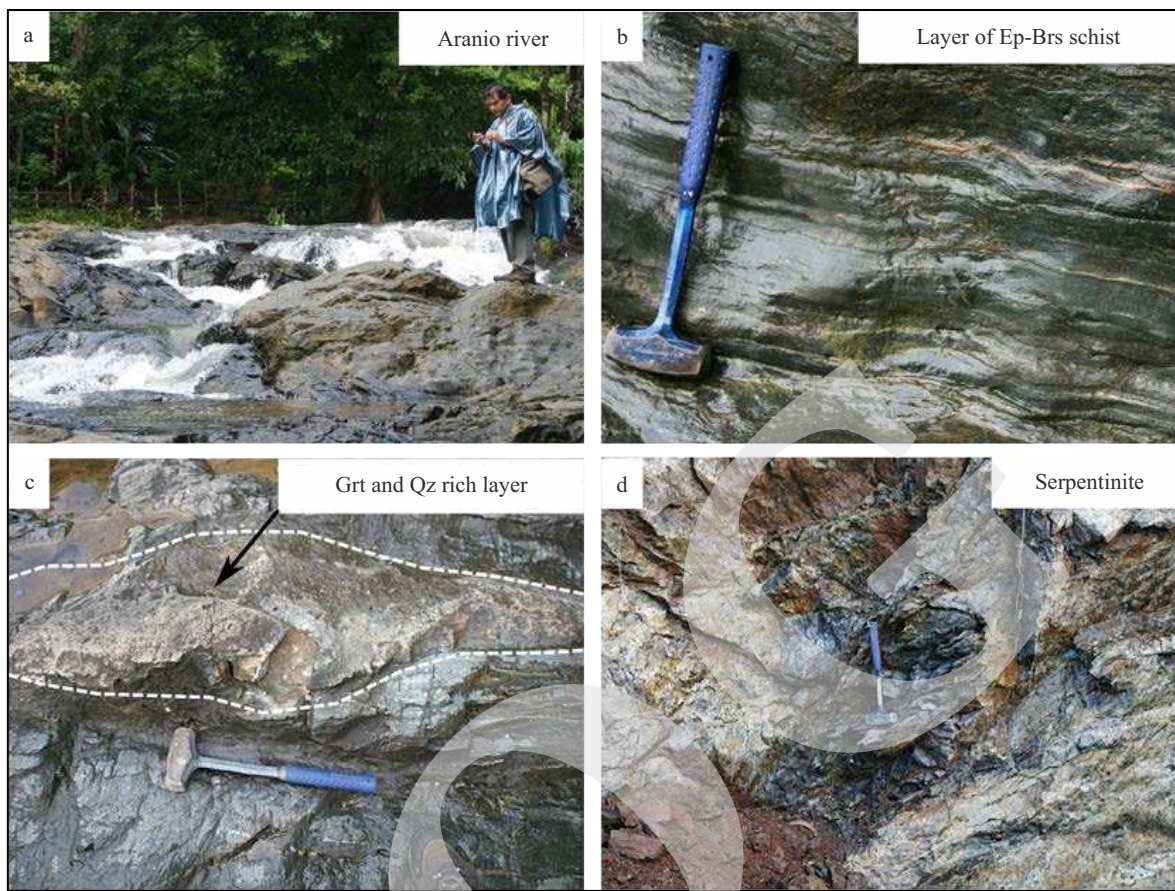
Figure 3. Modes of occurrence of the metamorphic rocks in the Meratus Complex, South Kalimantan. (a), Metamorphic rocks crop out along the Aranio River; (b), banded of epidote-barroisite schist; (c), garnet and quartz rich layer of garnet-bearing epidote- barroisite schist; (d), outcrop of serpentinite in Meratus Mountains.

the geological relationships between the schists and the serpentinites have not yet been clarified because of poor exposures due to deep weathering and heavily vegetated areas.

The mineral assemblages of collected samples are listed in Table 1. General petrographical characteristics of representative metamorphic rocks collected from the Meratus Complex are also described below. Fe^{3+} contents of garnet were calculated using algorithm suggested by Droop (1987). Phengite formulae have been calculated on the basis of eleven oxygen atoms with assuming all iron to be Fe^{2+}. Nomenclatures and calculated composition of the amphiboles follow Leake *et al.* (1997).

Epidote-barroisite schists

Epidote-barroisite schists show nematoblactic texture derived from the abundant barroisite and epidote (Figure 4a). The other assemblages are quartz, titanite, hematite, and apatite. Greenish blue barroisite nematoblast (XMg = 0.58 - 0.67, (Na + K)[A] = 0.15 - 0.31) is ~0.2 mm in length. Glaucophane (XMg = 0.61, (Na + K)[A] = 0.11) grains are included into the barroisite, indicating precursor blueschist-facies metamorphism. Quartz and titanite are also included into the barroisite. Chlorite replaces barroisite and other minerals along the cracks which indicates secondary phases.

Garnet-bearing epidote-barroisite schists

These rocks have fine-grained garnet (0.1 - 0.5 mm in diameter) along with epidote, barroisite, titanite, quartz, albite, and phengite, with or without apatite (Figure 4b). Granoblastic garnet (Prp11-18Alm53-60Sps8-10Grs14-24) has inclusions of quartz and epidote. Nematoblastic

Table. 1. Collected Metamorphic Rock Samples from the Meratus Complex and their Mineral Assemblages

No	Rock types	Major Mineral											Minor Mineral					Others	Secondary
		Grt	Gln	Ph	Qz	Ms	Hbl	Ep/Zo	Na-Ca amp	Pl/Ab	Srp	Act	Rt	Ttn	Hem	Spl	Chl		
1	Grt-bg Ep-Brs schist	Δ	±	Δ	◊	–	–	○	○	□	–	□	□	Δ	–	–	–	Ap	Chl, Ab, Cal
2	Ep-Brs schist	–	±	Δ	Δ	–	Δ	○	◊	□	–	□	□	Δ	–	–	–	Ap	Chl, Ab, Cal
3	Gln-Qz schist	–	□	Δ	◊	–	–	Δ	–	□	–	–	□	□	–	–	–	Ap	Ab, Chl, Cal
4	Grt-Ms schist	Δ	±	–	□	Δ	–	Δ	–	Δ	–	□	□	Δ	□	–	–	Ap	Ab, Chl
5	Act-Tlc schist	–	–	–	–	Δ	–	–	–	–	–	Δ	–	–	Δ	–	–	Tlc	Chl
6	Ep schist	–	–	–	◊	–	–	◊	–	–	–	–	–	–	Δ	–	–	Ap	
7	Ms schist	–	–	–	◊	○	–	–	–	–	–	–	–	–	Δ	–	–	Ap	Chl
8	Serpentinite	–	–	–	±	–	–	–	–	–	◊	–	–	–	–	Δ	□	Ol, Cpx	

◊ Abundant, ○ rich, Δ moderate, □ poor - absent, ± occur only in some samples, ( ) only as inclusion or relict; Act = actinolite; Tlc = talc; Ap = apatite; Chl = chlorite; Ab = albite; Cal = calcite; Cpx = clynopyroxene; ol = olivine; Grt = garnet; Gln = glaucophane; Ph = phengite; Qz = quartz; Ms = muscovite; Hbl = hornblende; Ep = epidote; Srp = serpentine; Rt = rutile; Ttn = titanite.

barroisite (0.1 - 0.3 mm in length; XMg = 0.62-0.67, (Na + K)[A] = 0.23 - 0.35), epidote, and lepidoblastic phengite (~0.2 mm in lenght; XSi = 0.61 - 0.64) form schistosity in the rock. Some of them are replaced by chlorite and albite during retrograde metamorphism.

Epidote-glaucophane schists

These rocks mainly consist of glaucophane, quartz, epidote, phengite, and titanite with or without hematite and apatite (Figure 4c). Excluding quartz, glaucophane, phengite, and epidote are ubiquitous in matrix. Glaucophane (~0.25 mm in diameter; XMg = 0.64 - 0.67, [Na + K][A] = 0.02 - 0.77) and epidote (~0.2 mm in diameter) show sheaf texture and sometimes show random orientation. Several fine-grained phengites (<0.05 mm in diameter; XSi = 0.64 - 0.67) also show random orientation. Secondary chlorite, calcite, and albite replace glaucophane, phengite, and epidote along the cracks.

Garnet-muscovite schists

These rocks have porphyroblastic texture with numerous garnet porphyroblasts (Figure 4d). These samples mainly consist of garnet, muscovite, quartz, epidote, rutile, albite, and apatite. A lot of cracks appear in the coarse-grained garnet (0.5 - 1 mm in diameter). Those cracks are filled with chlorite and albite. Muscovite (~0.25 mm in diameter) and epidote (~0.3 mm in diameter) are abundant in the matrix. Those minerals develop the schistose fabric of these rocks. Secondary chlorite subsequently replaces garnet and other minerals by pseudomorph after them.

Tremolite-talc schist

This rock is rarely found in study area. It consists of tremolite, talc, and quartz (Figure 4e). Sheaf texture of tremolite (~0.5 mm in diameter) is embedded in the abundant talc grains. Interstitial albite and quartz occur filling in the cracks.

Serpentinite

Serpentinite preserves relict mineral phases. Clinopyroxene and olivine are well recognized under polarized microscope despite suffering from crosscut by mesh texture of serpentine (Figure 4f). Spinel (0.2 - 0.5 mm in diameter) occurs in the matrix which consider as a relict mineral.

Petrography and Mineral Chemistries of Garnet-bearing epidote-barroisite Schist

The estimation of P-T paths of the high-pressure metamorphic rock (garnet-bearing epidote-barroisite schist; Sample no. 031601) from the Meratus Complex is described in detail in this section. The estimated metamorphic evolution in this chapter could reflect the evolution of the Meratus Complex of South Kalimantan. General petrography of the rock sample discussed here has already been described in the previous section. Hence, in this section, the description of petrography and mineral chemistry will focus on the selected garnet-bearing epidote-barroisite schist sample with mineral coexistence on that is mainly described in detail.
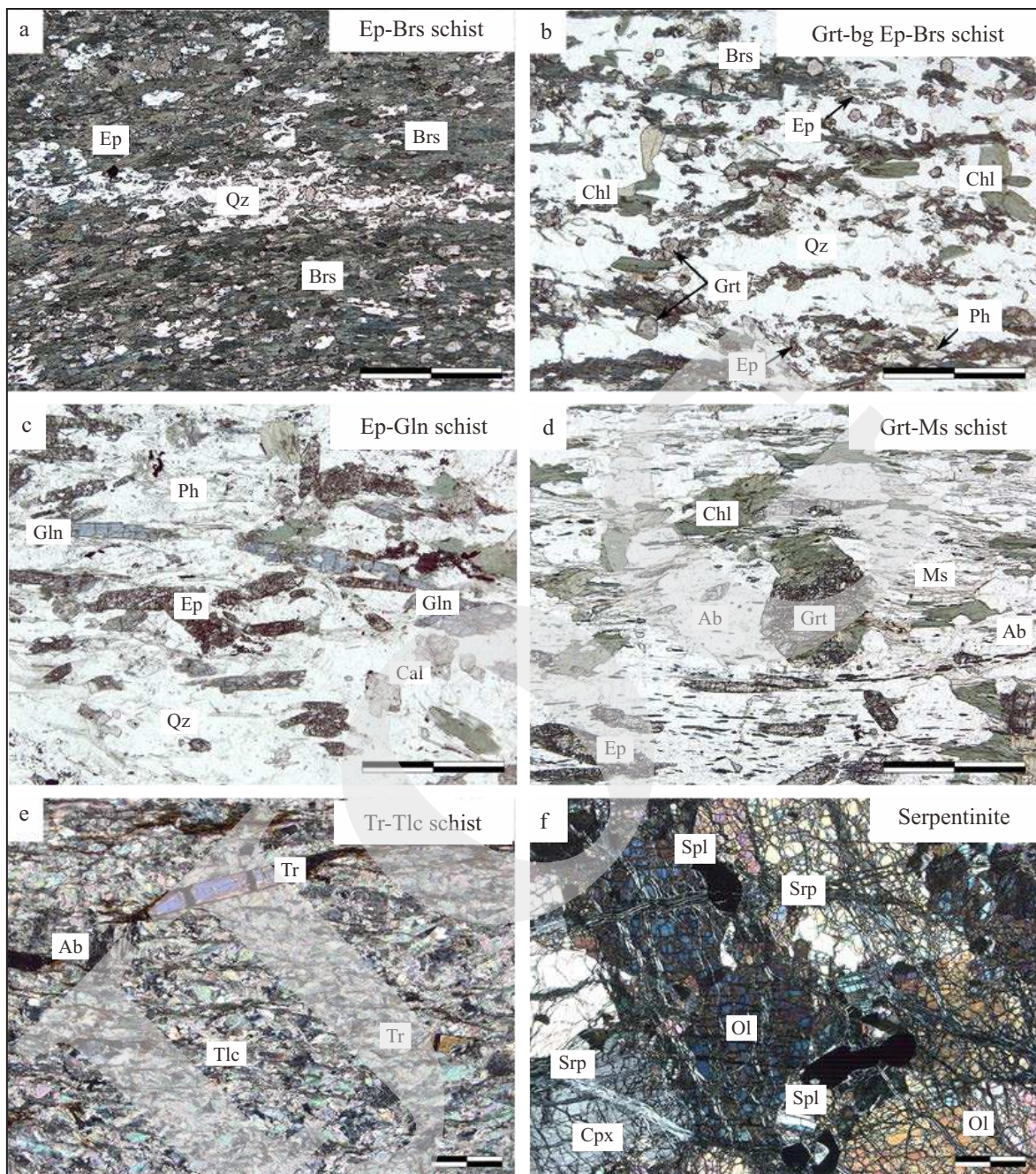
Figure 4. Photomicrographs of metamorphic rocks from Meratus Complex. (a), Foliation of epidote-barroisite (Ep-Brs) schist; (b), foliation of garnet-bearing epidote-barroisite (Grt-bgEp-Brs) schist; (c), bluish elongated glaucophane (Gln) occur with epidote (Ep), phengite (Ph), and quartz (Qz); (d) garnet- muscovite (Grt-Ms) schist with secondary chlorite (Chl) pseudomorph after garnet (Grt); (e), nematoblastic actinolite within matrix talk in tremolite-talc (Tr-Tlc) schist; (f) mesh texture in serpentinite (Srp) with relict olivine (Ol) and clinopyroxene (Cpx). The scale bar without expression in each of photomicrograph on this publication indicates 1 mm.

Detailed petrography

The garnet-bearing epidote-barroisite schist can be subdivided into garnet-bearing and -free domains. On the garnet-bearing domain, fine-grained garnet, epidote, barroisite, titanite, quartz, and phengite coexist (Figure 5a). In the garnet-free domain; barroisite, epidote, titanite, quartz, albite, and phengite coexist. The schistosity of this rock is mainly defined by barroisite, phengite (~0.2 mm), and epidote (~0.15 mm). Core portion of

fine-grained garnet (0.1 - 0.5 mm) has inclusions of quartz, titanite, apatite, chlorite, and epidote (Figure 5b). Blue- greenish barroisites (0.5 - 1 mm) show compositional heterogeneity suggested by patchy texture of Si-rich and Si-poor barroisites (Figure 5c). In several grains, thin layer of actinolite rims the barroisites (Figure 5d). Some of the barroisites are replaced by chlorite and albite, which indicate secondary phases in this rock.

Mineral chemistry

Mineral chemistries of the garnet-bearing epidote-barroisite schist are described in detail. The analyses were performed using the same system as described in the previous section. Representative mineral chemistry analyses of the garnet-bearing epidote-barroisite schist are presented in Table 2.

Garnet

Euhedral garnet obviously has two domains defined by a different composition, which show core and rim portions (Figure 6). The garnet has a barrier reef type zoning pattern identified by an irregular/anhedral shape of core portion (Figure 6). Enami *et al.* (2011) studied the barrier reef garnet grains from Myanmar eclogite and they suggested that relics of an older core occurring as fragments were dissolved by the new garnet. The chemical zoning on the garnet is clearly identified on the Ca, Fe, Mg, and slightly on the Mn elements (Figure 6). Epidote, titanite, and apatite are inclusions in the core portion of garnet which are clearly identified particularly by Ca and Ti elements (Figure 6). Based on the chemical zonation (rim to core),
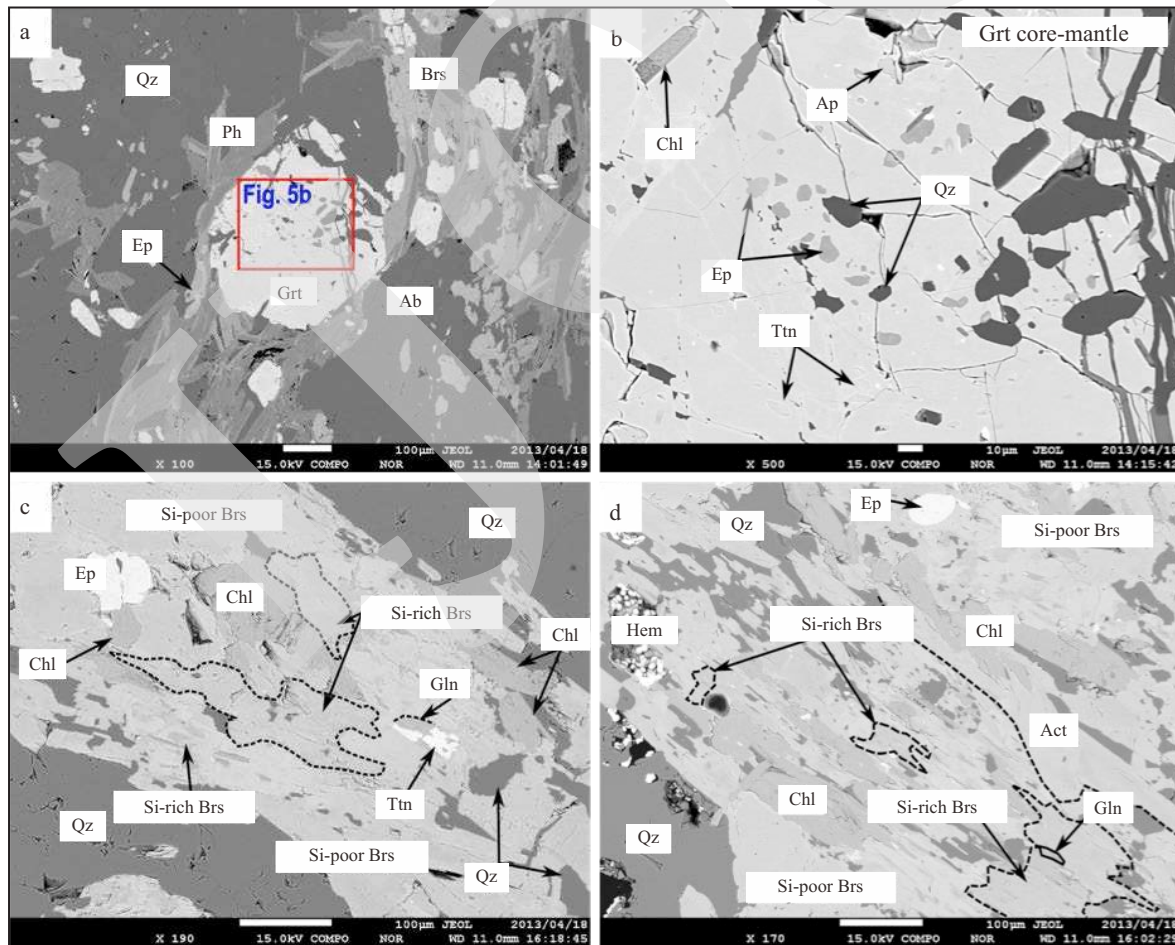

Figure 5. Back-scattered electron images of garnet-bearing epidote-barroisite schist. (a) and (b) quartz (Qz), epidote (Ep), titanite, apatite, and chlorite (Chl) included in the hypidiomorphic garnet grain. (c) and (d) barroisites (Brs) have relict spot of Si-rich with glaucophane (Gln) inclusions. Several grains have thin layer of actinolite (Act) on the rim portion.

Table 2. Representative Microprobe Analyses of Garnet, Phengite, Amphibole, Epidote, and Titanite

Mineral	Garnet		Phengite		Amphibole				Epidote		Ttn
Position	core	rim ↑	I	II↑	inc	matrix I	matrix II	rim	inc↕	matrix	inc↕
SiO_2	37.75	38.29	46.11	51.38	53.57	49.05	42.15	52.05	37.51	38.10	30.76
TiO_2	0.18	0.05	0.62	0.09	0.22	0.16	0.68	0.07	0.17	0.08	36.24
Al_2O_3	21.38	21.34	29.97	24.29	5.84	7.05	13.15	3.20	25.35	25.89	2.25
Cr_2O_3	0.00	0.00	0.06	0.03	0.10	0.03	0.05	0.03	0.00	0.00	0.02
FeO	24.39	27.84	3.18	3.09	17.62	19.23	19.93	16.37	-	-	-
Fe_2O_3	-	-	-	-	-	-	-	-	10.42	9.69	2.07
MnO	4.58	3.27	0.05	0.09	0.27	0.42	0.28	0.33	0.45	0.22	0.42
MgO	2.61	4.62	1.68	3.56	9.75	9.88	7.43	13.43	0.11	0.01	0.09
CaO	9.51	5.20	0.00	0.00	3.92	8.16	9.83	10.07	22.70	23.63	26.98
Na_2O	0.04	0.02	1.12	0.14	5.35	3.18	3.00	1.71	0.00	0.02	0.04
K_2O	0.00	0.03	9.64	10.93	0.08	0.25	0.95	0.11	0.00	0.02	0.01
Total	100.43	100.65	92.43	93.59	96.72	97.39	97.44	97.36	96.69	97.66	98.87
O	12	12	11	11	23	23	23	23	12.5	12.5	5
Si	2.98	3.00	3.20	3.51	7.72	7.19	6.36	7.53	2.99	3.00	1.02
Ti	0.01	0.00	0.03	0.00	0.02	0.02	0.08	0.01	0.01	0.00	0.90
Al	1.99	1.97	2.45	1.96	0.99	1.22	2.34	0.55	2.38	2.41	0.09
Cr	0.00	0.00	0.00	0.00	0.01	0.00	0.01	0.00	0.00	0.00	0.00
Fe^{3+}	0.00	0.00	0.00	0.00	0.79	0.85	0.55	0.76	0.63	0.57	0.06
Fe^{2+}	1.61	1.83	0.18	0.18	1.33	1.51	1.97	1.21	0.00	0.00	0.00
Mn	0.31	0.22	0.00	0.01	0.03	0.05	0.04	0.04	0.03	0.01	0.01
Mg	0.31	0.54	0.17	0.36	2.10	2.16	1.67	2.90	0.01	0.00	0.00
Ca	0.80	0.44	0.00	0.00	0.61	1.28	1.59	1.56	1.94	2.00	0.96
Na	0.01	0.00	0.15	0.02	1.49	0.90	0.88	0.48	0.00	0.00	0.00
K	0.00	0.00	0.85	0.95	0.01	0.05	0.18	0.02	0.00	0.00	0.00
Total cation	8.02	8.01	7.05	6.99	15.11	15.23	15.65	15.06	7.99	8.00	3.04
Prp (%)	10.12	17.89	-	-	-	-	-	-	-	-	-
Alm (%)	53.18	60.45	-	-	-	-	-	-	-	-	-
Sps (%)	10.12	7.20	-	-	-	-	-	-	-	-	-
Grs (%)	26.58	14.46	-	-	-	-	-	-	-	-	-
Si/(Si + Al)	-	-	0.57	0.64	-	-	-	-	-	-	-
Na/(Na+K)	-	-	0.15	0.02	-	-	-	-	-	-	-
Na/(Na + Ca)	-	-	-	-	0.71	0.41	0.36	0.23	-	-	-
$Mg/(Mg + Fe^{2+})$	0.56	0.69	0.97	0.98	0.92	0.91	0.89	0.93	-	-	-
$Fe^{3+}/(Fe^{3+} + Al)$	-	-	-	-	-	-	-	-	0.21	0.19	0.39

↑ and ↕ = Pair data used for calculation P-T condition.

the garnet core portion has increased in grossular and decreased in almandine and pyrope (Prp10-15Alm53-58Sps8-11Grs18- 24; Figure 7). The rim portion of the garnet shows increasing pyrope and almandine but decreasing grossular with spessartine that are relatively flat (Prp16-18Alm59-61Sps7-10Grs13-16; Figure 7). The increasing spessartine components along the garnet cracks (Sps18-20) might be an effect of retrograde metamorphism.

Phengite

Two types of phengite were recognized in the matrix (phengites 1 and 2). The differences between both phengites are obviously identified by the chemical mapping images of Na, Fe, Mg, Al, and Si elements (Figure 8). The phengite 1 is richer in Na and Al but lesser in Si, Mg, and K elements (XNa = 0.141-0.151; XSi = 0.566-0.571; XMg = 0.480-0.528; Figure 9a), whereas phengite 2 has higher XSi values in the core (XNa = 0.019-
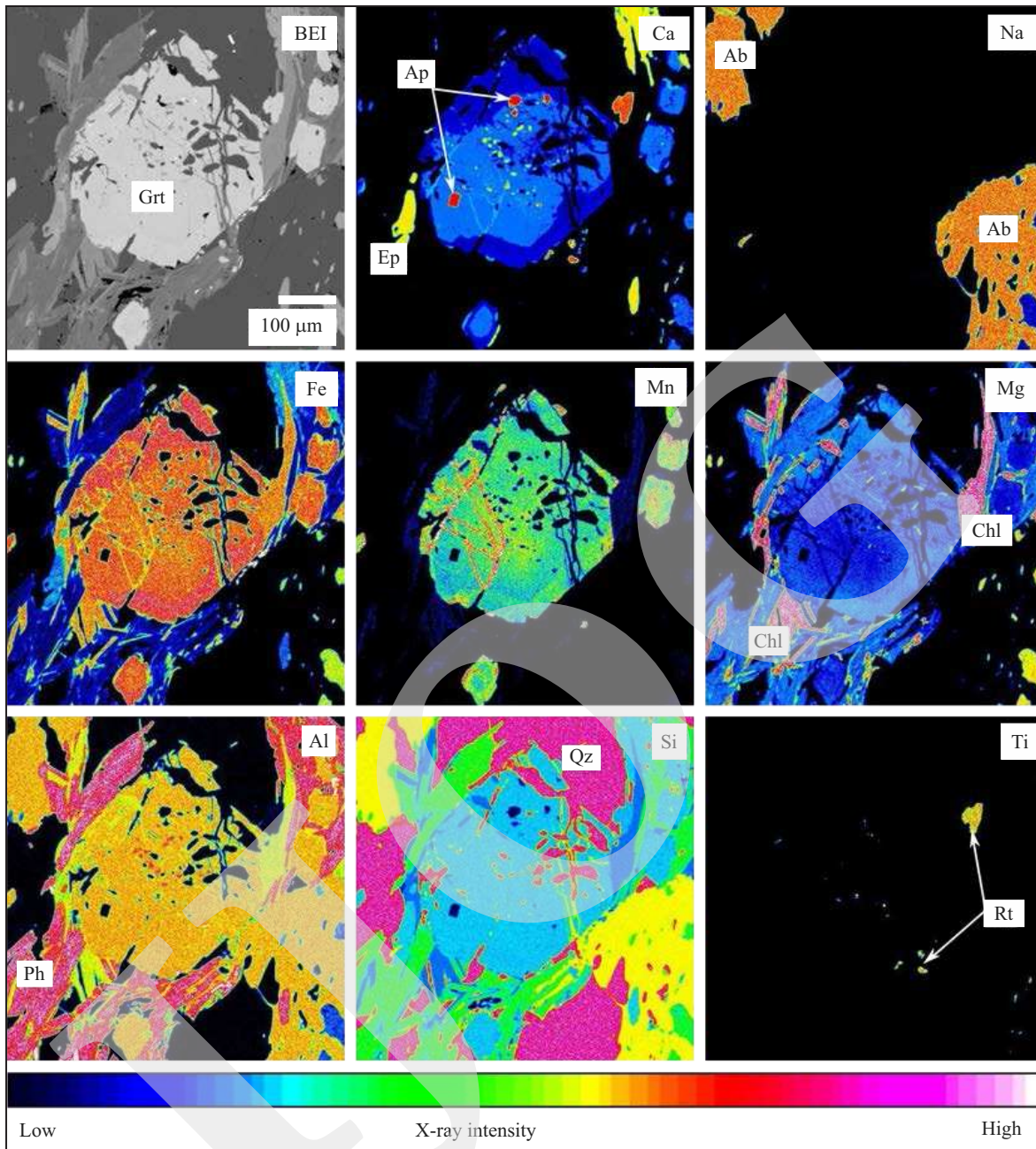
Figure 6. Back-scattered and chemical mapping images on the garnet in garnet-bearing epidote-barroisite schist from Meratus Complex on the response of Ca, Na, Fe, Mn, Mg, Al, Si, and Ti elements. The chemical zoning on the garnet is clearly identified on the Ca, Fe, Mg, and slightly on the Mn elements. The garnet has a barrier reef type zoning pattern which is identified by an irregular/anhedral shape of core-portion clearly identified in Ca component. Mn components increase along the garnet cracks that might indicate a secondary stage. Grt = garnet; Ap = apatite; Ep = epidote; Chl = chlorite; Ab = albite; Ph = phengite.

0.044; $XSi = 0.618$-0.642; $XMg = 0.572$-0.677; Figure 9b).

Amphibole

Amphiboles occur as lepidoblast in the matrix. The internal textures of amphiboles are obviously identified in the back-scattered images

(Figures 5c, d). Barroisites patch with higher- Si contents ($Si = 7.05$ - 7.23; $XMg = 0.58$ - 0.60; $Na[B] = 0.70$ - 0.87; hereafter called barroisite I) included in coarse-grained Si-poor barroisite grain (barroisite II) with composition ranging $Si = 6.39$ - 6.88, $XMg = 0.46$ - 0.57, and $Na[B] = 0.41$ - 0.75 (Figures 5c-d, 10. Rarely Na-rich am-
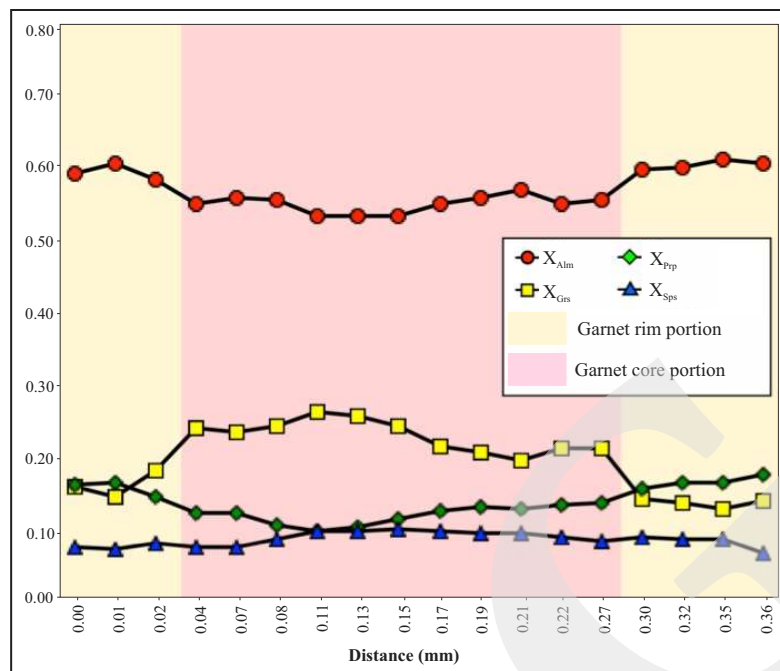
Figure 7. Chemical composition of zoning profile from core to rim in garnet. The garnet core portion has higher grossular and lower almandine and pyrope. Rim portion shows increasing pyrope and almandine but decreasing grossular with spessartine which are relatively flat.

phiboles are also included in the barroisite, which are plotted in the winchite and glaucophane fields (Si = 7.72 - 7.81; XMg = 0.61 - 0.63; Na[B] = 1.40 - 1.60; Figures 5c-d, 10). Thin layer of actinolite rims the barroisites in the matrix which have richer-Si and lower-Na[B] components. Those are with composition ranging Si = 7.42 - 7.69, XMg = 0.62 - 0.70, and Na[B] = 0.44 - 0.82 (Figures 5c-d, 10).

Other minerals

Other minerals are epidote, titanite, chlorite, and albite. Those are describing in here. There are no significant differences between epidotes that occur as the inclusion and in the matrix. Both of them have similar ranges of pistacite contents (XFe^{3+} = 0.18 - 0.30). Titanite as inclusion in garnet core have higher-XAl (0.084 - 0.275) than titanite in the matrix (XAl = 0.084 - 0.275). Chlorite occurring along cracks of garnet and replacing other minerals has a compositional range of XFe = 0.44 - 0.46. Albite occur as interstitial phases along the cracks of barroisite and in the matrix has composition of XAb = 0.98 - 1.00.

DISCUSSION OF P-T ESTIMATION

Based on the textural and mineral chemical results, the metamorphic evolution of the garnet-bearing epidote-barroisite schist is divided into three stages which represents the different metamorphic facies as follows: prograde (blueschist-facies), peak (amphibolite-facies), and retrograde stages (greenschist-facies). Summary of mineral assemblages and their chemical characters are presented in Table 3.

Prograde Stage

The prograde stage of garnet-bearing epidote-barroisite schist might be preserved as mineral inclusions, composed of glaucophane that is included in the barroisite in the matrix and the epidote in the garnet core. As described previously, two kinds of phengite were identified in the matrix (Figure 8) which are Na-rich phengite (phengite 1) and normal phengite (phengite 2). The Na-rich phengite (phengite 1) might be pseudomorph after paragonite. Hence, the primary stage of this rock might be represented by the assemblage of glaucophane + epidote ± paragonite (Table 3).
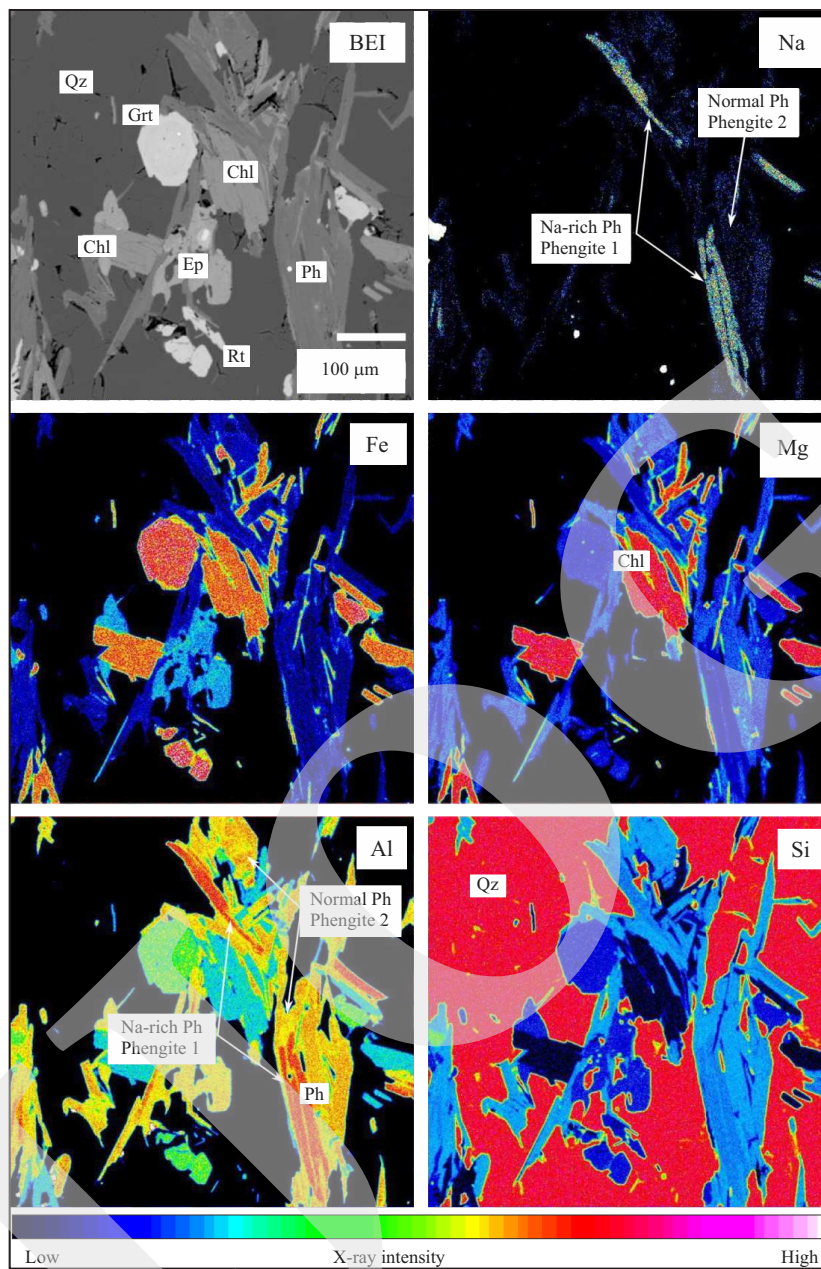
149

Figure 8. Back-scattered and chemical mapping images on the phengite on the response of Na, Fe, Mg, Al, and Si. Two kinds of phengites are identified; Na-rich phengite (phengite 1) and normal phengite (phengite 2). Abbreviations see Figure 7.

The equilibrium reaction of $Lws + Jd = Pg + Ep/Zo + Qz + H_2O + Vapor$ from Heinrich and Althaus (1988) might give a minimum temperature for primary stage as lawsonite and Na-clinopyroxene that could not be found in this rock (Figure 11). The presence of glaucophane grains included in the barroisite can be used to constrain the maximum temperature of prograde stage. The maximum temperature of glaucophane is based on experimental studies of natural glaucophane

by Maresch (1977) at temperature 550 ºC above 1.0 GPa (Figure 11). Therefore, petrogenetic grid from Evans (1990) suggests the primary stage occupies the epidote blueschist-facies stability field (Figure 11; Table 3).

Titanite and epidote grains are included in the garnet core (Figure 5b). Rutile, which is not observed in the garnet inclusion, appears in the matrix. Manning and Bohlen (1991) suggested geobarometry involving titanite, rutile, epidote
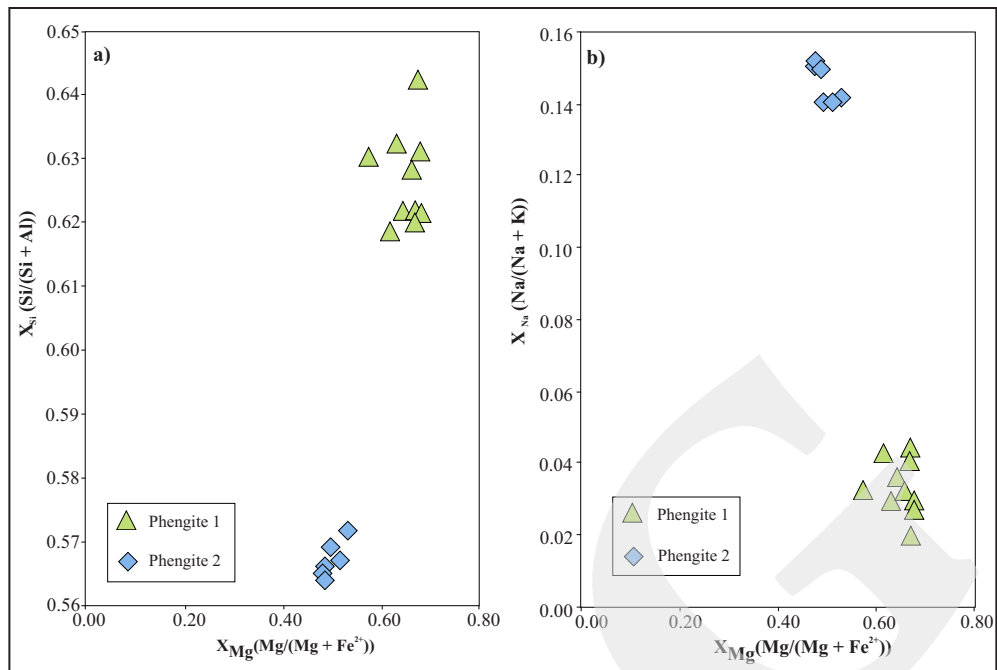
Figure 9. Chemical characteristics of phengite grains. Phengites 1 and 2 are plotted on the [a] XSi *vs.* XMg and [b] XNa *vs.* XMg.
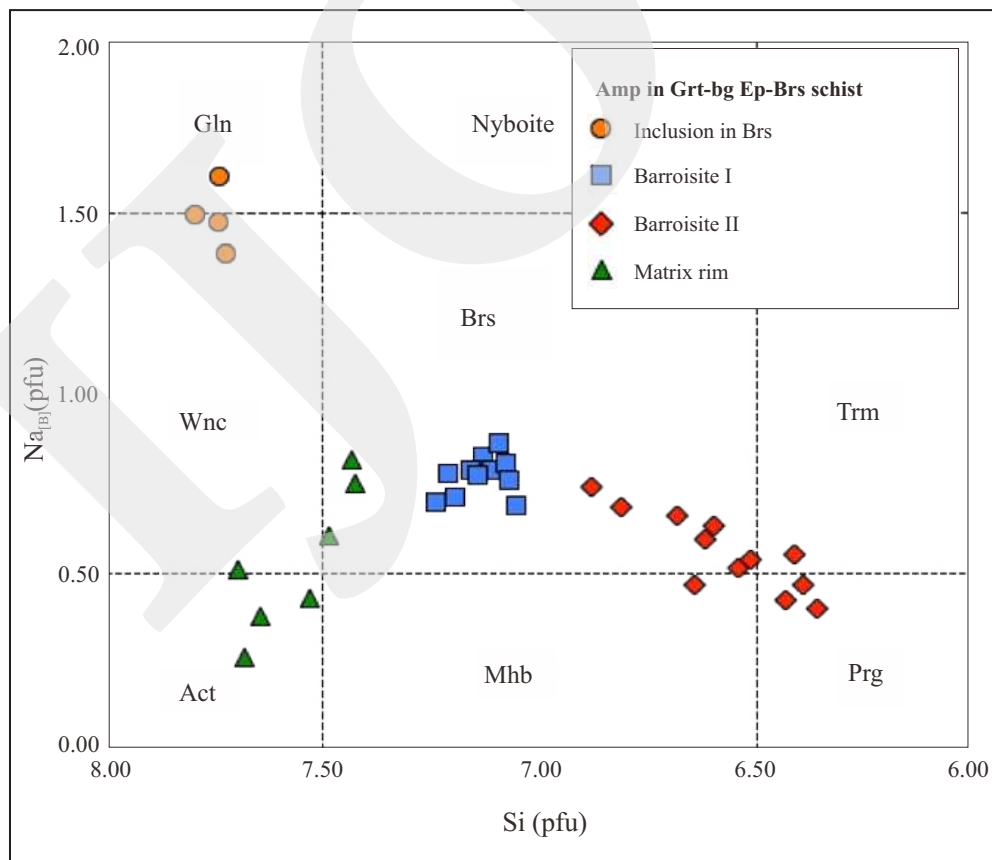

Figure 10. Compositional ranges of amphibole grains. Amphibole (Amp) grains included in the barroisite (Brs) are alkali amphibole straddling in the glaucophane (Gln) and winchite (Wnc) fields. Amphibole grains occuring in the matrix are barroisite and several grains straddle on the magnesio-hornblende (Mhb)/pargasite (Prg)/taramite (Trm) fields. Matrix rim rich in Si content but lower Na[B]. Those straddle in the barroisite/winchite/actinolite fields.

Table 3. Mineral Parageneses in Metamorphic Evolution of Garnet-bearing Epidote-barroisite Schist

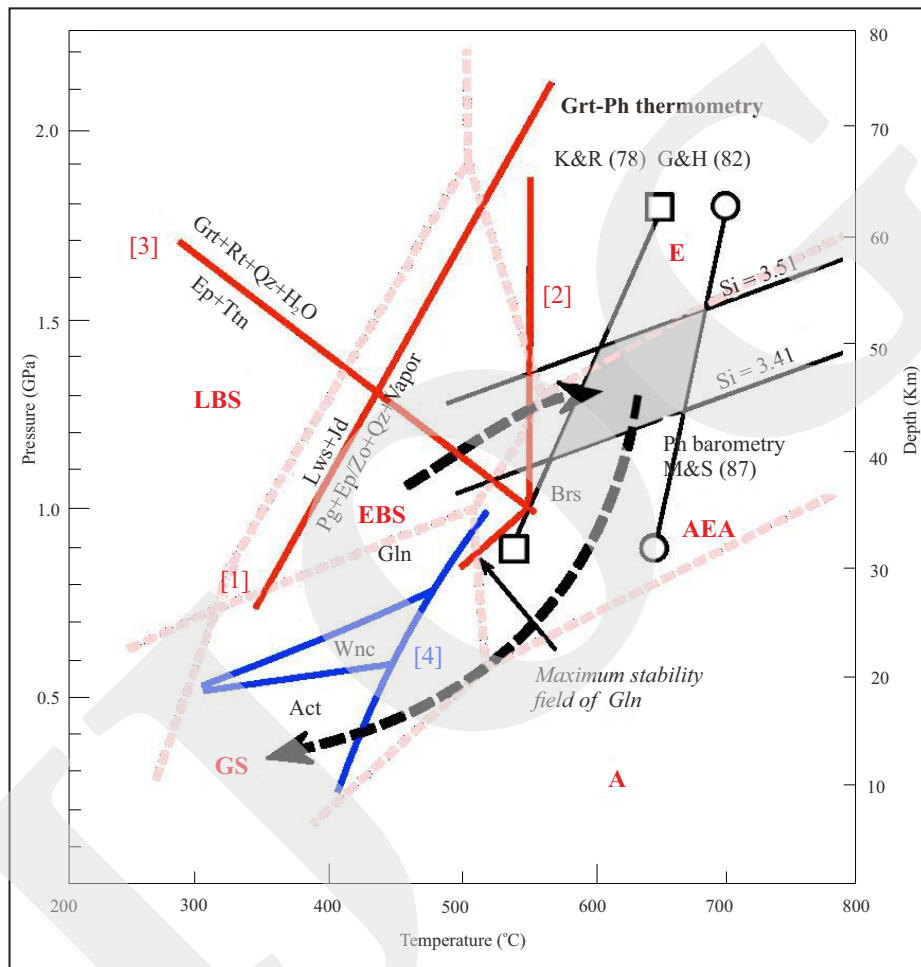| Stage	Metamorphic Facies	Mineral Parageneses
Prograde	Blueschist	Grt (core) + Ep + Ttn + Gln + Ph 1(relict Pg) + Qz
Peak	Amphibolite	Grt (rim) + Brs (Si-rich) + Ph 2 + Qz + Ep + Hem + Rt + Chl ± Ab
Retrograde 1	Greenschist	Si-poor Amp + Ttn + Qz ± Ep ± Chl ± Ab
Retrograde 2	Greenschist	Act + Ab + Chl + Qz

*Abbreviations see Table 1.

Figure 11. P-T diagram of garnet-bearing epidote-barroisite schist. The petrogenetic grids are from Evans (1990), the abbreviations as follows; LBS: lawsonite blueschist-facies, E: eclogite-facies, AEA: albite epidote amphibolite-facies, A: amphibolite-facies, GS: greenschist-facies. Experimental determined reactions: [1] Lws + Jd = Pg + Ep/Zo + Qz + Vapor (Heinrich and Althaus, 1988) [2] maximum stability field of glaucophane (Maresch, 1997), [3] Ep + Ttn = Grt + Rt + Qz + H2O (Manning and Bohlen, 1991), and [4] amphiboles solid-solution (Otsuki and Banno, 1990). Garnet-phengite geothermometry: open square from Krogh and Raheim (1978) and open circle from Green and Hellman (1982). Geobarometry of phengite from Massonne and Schreyer (1987).

and grossular in eclogite was based on dehydration reaction of Ep + Ttn = Grs + Rt + Qz + H_2O. Garnet in this sample does not show an increase of grossular between core and rim. However, if other net-transfer reaction producing pyrope and almandine, sometimes the grossular weight % does not show increasing although it may be produced by that reaction. The equilibrium of titanite, epidote, and grossular in the garnet core was observed (Table 3). The activity of grossular component in garnet core was calculated from the mixing model of Berman (1990). The titanite,

clinozoisite/epidote, rutile, quartz, and H_2O activities were calculated following Manning and Bohlen (1991). Activity of titanite (Table 2) was calculated as $X_{ca}X_{Ti}X_{Si}[X_o]^5$ with $X_o = (5 - X_{Al} - X_{Fe}^{3+})$ by assuming that F and OH substitutions were balanced by Al and Fe^{3+}, which correspond to $\alpha_{Tin} = 0.756$. The activity of clinozoisite/epidote was calculated as $X_{Ca}^2 X_{Al}^2 (1 - Fe^{3+})X_{Si}^3$ with the maximum pistacite selected (Table 2) to give the maximum pressure corresponding to $\alpha_{Czo} = 0.367$. Other activities of rutile, quartz, and H_2O are assumed to be 1 (Manning and Bohlen, 1991). The activities of the assemblage yield 1.7 - 1.0 GPa for an assumed temperature of 300 - 550 ºC interpreted as the maximum pressure limit of the prograde stage (Figure 11).

Peak Stage

Mineral coexistences at the peak P-T condition are garnet rim, barroisite, phengite 2, epidote, and quartz (Table 3). The temperature condition is estimated using the garnet-phengite geothermometer formulated by Krogh and Raheim (1978) and Green and Hellman (1982). The results give temperature ranges of 547 - 636 ºC assuming 1.0 GPa (Figure 11). The peak pressures are estimated using phengite geobarometer formulated from Massone and Schreyer (1980). Maximum and minimum Si contents on phengite 2 are used for this geobarometer to obtain maximum and minimum pressures, respectively. The result gives a range of pressures at 1.1 - 1.5 GPa. Petrogenetic grid from Evans (1990) suggests that this peak P-T conditions are plotted on the epidote amphibolite-facies (Figure 11).

Retrograde Stage

The retrograde decompression stages in this rock are represented by textural relations of amphiboles in the matrix (Figures 5c - d). Following solid-solution diagram of amphiboles from Otsuki and Banno (1990), the retrograde P-T path is explained by changing chemical composition of amphiboles from Si-Na rich barroisite to actinolite rim through Si-Na poor amphiboles (barroisite II; Figures 5c-d, 11). Therefore, there are two stages in the retrograde metamorphism. The second or last retrograde-decompression P-T path should be on the stability field of actinolite (Table 3) which lies near 0.5 GPa at 350 ºC (Figure 11).

Metamorphic Evolution

The pressure-temperature path of garnet-bearing epidote-barroisite schist was estimated by using mineral parageneses, reaction textures, and mineral chemistries. The obtained pressure-temperature path of the garnet-bearing epidote-barroisite schist has a clockwise trajectory. The rock experienced primary stage on the stability field of paragonite + glaucophane + epidote and subsequent increasing pressure and temperature to the stability field of barroisite, which peak P-T condition of this rock was at 547 - 690 ºC and 1.1 - 1.5 GPa on the albite epidote amphibolite-facies that correspond to the depth of 50 - 60 km. The retrograde stage is presented by changing mineral compositions of amphiboles from the Si-rich barroisite- to the actinolite-stability field through Si-poor barroisite/magnesio-hornblende/taramite/pargasite, which lies near 0.5 GPa at 350 ºC.

CONCLUSIONS

It might be concluded that metamorphic rocks from the Meratus Complex experienced high-pressure condition of the epidote blueschist-facies before the peak metamorphism of the epidote-amphibolite facies. The worldwide blueschist-facies metamorphic rock is consided as markers of fossil subduction zones. As already mentioned before, the K-Ar dating of various mica schists in this location yielded ages ranging 110 - 180 Ma, which are in the similar age with the metamorphic rocks in South Sulawesi and Central Java. Therefore, the occurrences of prograde blueschist-facies in Meratus Complex might be concluded that this area was originally in subduction zone during Cretaceous age.

Compared to the other high-pressure metamorphic terranes in central Indonesia (*e.g.* eclogite from Bantimala Complex: 580 - 650 ºC at 1.8 - 2.4 GPa and 630 - 700 ºC at 2.9 - 3.1 GPa and eclogite from Luk Ulo Complex: 2.0-2.3 GPa at 365 - 410 ºC and 2.15 - 2.25 GPa at 550 - 625 ºC, the estimated P-T metamorphic condition of garnet-bearing epidote-barroisite schist from the Meratus Complex has a lower peak pressure but giving higher temperature (547 - 690 ºC) at pressure 1.1 - 1.5 GPa. The high-pressure metamorphic rocks from Bantimala and Luk Ulo Complexes are characterized by low- to very low geothermal gradients. Furthermore, this study shows that garnet-bearing epidote-barroisite schist from the Meratus Complex has a higher geothermal gradient compared to the other metamorphic terranes. Possibly, the Meratus Complex was proximal and the others were distal with respect to the original Cretaceous subduction site. The results reported here and further precise petrological and geochronological studies will contribute toward a better understanding of the Mesozoic tectono-metamorphic development of the eastern margin of the Sundaland.

References

Asikin, S., Handoyo, A., Busono, A., and Gafoer, S., 2007. *Geological map of the Kebumen Quadrangles, Jawa; Scale 1:100,000.* Geological Research and Development Centre of Indonesia. Bandung.

Berman, R.G., 1990. Mixing properties of Ca-Mg-Fe-Mn garnets. *American Mineralogist*, 75, p.328-344.

Droop, G.T.R., 1987. A general equation for estimating Fe^{3+} concentrations in ferromagnesian silicates and oxides from microprobe analyses, using stoichiometric criteria. *Mineralogical Magazine*, 51, p.431-435.

Enami, M., Ko, Z.W., Win, A., and Tsuboi., 2011. Eclogite from the Kumon range, Myanmar: Petrology and tectonic implications. *Gondwana Research*, 21, p.548-558.

Evans, B.W., 1990. Phase relations of epidote-blueshists. *Lithos*, 25, p.3-23.

Green, T.H. and Hellman, P.L., 1982. Fe-Mg partitioning between coexisting garnet and phengite at high pressure, and comments on a garnet-phengite geothermometer. *Lithos*, 15, p.253-266.

Heinrich, H. and Althaus, E., 1988. Experimental determination of the 4 lawsonite + 1 albite = 1 paragonite + 2 zoisite + 2 quartz + 6 H_2O and 4 lawsonite + 1 jadeite = 1 paragonite + 2 zoisite + 2 quartz + 6H_2O. *Neues Jahrbuch Mineral Monatsh*, 11, p.516-528.

Kadarusman, A. and Parkinson, C.D., 2000. Petrology and P-T evolution of garnet peridotites from central Sulawesi, Indonesia. *Journal of Metamorphic Geology*, 18, p.193-209.

Kadarusman, A., Miyashita, S., Maruyama, S., Parkinson, C.D., and Ishikawa, A., 2004. Petrology, geochemistry and paleogeographic reconstruction of the East Sulawesi Ophiolite, Indonesia. *Tectonophysics*, 392, p.55-83.

Kadarusman, A., Massonne, H.J., Roermund, V.H., Permana, H., and Munasri., 2007. P-T evolution of eclogites and blueschists from the Luk Ulo Complex of Central Java, Indonesia. *International Geology Review*, 49, p.329-356.

Krogh, E.J. and Raheim, A., 1978. Temperature and pressure dependence of Fe-Mg partitioning between garnet and phengite, with particular reference to eclogite. *Contributions to Mineralogy and Petrology*, 66, p.75-80.

Leake, B.E., Woolley, A.R., Arps, C.E.S., Birch, W.D., Gilbert, M.C., Grice, J.D., Hawthorne, F.C., Kato, A., Kisch, H.J., Krivovichev, V.G., Linthout, K., Laird, J., Mandarino, J.A., Maresch, W.V., Nickel, E.H., Rock, N.M.S., Schumacher, J.C., Smith, D.C., Stephenson, N.C.N., Ungaretti, L., Whittaker, E.J.W., and Youzhi, G., 1997. Nomenclature of amphiboles: report of the subcommittee on amphiboles of the International Mineralogical Association, Commission on New Minerals and Mineral Names. *The Canadian Mineralogist*, 35, p.219-246.

van Leeuwen, T., Allen, C.M., Kadarusman, A., Elburg, M., Palin, J.M., Muhardjo, and Suwijanto., 2006. Petrologic, isotopic, and radiometric age constraints on the origin and tectonic history of the Malino Metamorphic Complex, NW Sulawesi, Indonesia. *Journal of Asian Earth Sciences*, 29, p.751-777.

Manning, C.E. and Bohlen, S.R., 1991. The reaction titanite + kyanite = anorthite + rutile and titanite-rutile barometry in eclogites. *Contributions to Mineralogy and Petrology*, 109, p.1-9.

Marresch, W.V., 1977. Experimental studies on glaucophane: an analysis of present knowledge. *Tectonophysics*, 43, p.109-125.

Maruyama, S., Liou, J.G., and Terabayashi, 1996. Blueschist and eclogites of the world and their exhumation. *International Geology Review*, 38, p.485-594.

Massone, H.J. and Schreyer, W., 1987. Phengite geobarometry based on the limiting assemblage with K-feldspar, phlogopite, and quartz. *Contributions to Mineralogy and Petrology*, 96, p.212-214.

Miyazaki, K., Zulkarnain, I., Sopaheluwakan, J. and Wakita, K., 1996. Pressure-temperature conditions and retrograde paths of eclogites, garnet-glaucophane rocks and schists from South Sulawesi, Indonesia. *Journal of Metamorphic Geology*, 14, p.549-563.

Miyazaki, K., Sopaheluwakan, J., Zulkarnain, I., and Wakita, K., 1998. Jadeite-quartz- glaucophane rock from Karangsambung, Central java, Indonesia and its tectonic implications. The Island Arc, 7, p.223-230.

Otsuki, M. and Banno, S., 1990. Prograde and retrograde metamorphism of hematite-bearing basic schists in the Sanbagawa belt in central Shikoku. *Journal of Metamorphic Geology*, 8, p.425-439.

Parkinson, C.D., 1998. An outline of the petrology, structure, and age of the Pompangeo schist Complex of central Sulawesi, Indonesia. *The Island Arc*, 7, p.231-245.

Parkinson, C.D., Miyazaki, K., Wakita, K., Barber, A.J., and Carswell, A., 1998. An overview and tectonic synthesis of the pre-Tertiary very-high-pressure metamorphic and associated rocks of Java, Sulawesi and Kalimantan, Indonesia. *The Island Arc*, 7, p.184-200.

Setiawan, N.I., 2013. *Metamorphic evolution of central Indonesia*. PhD Thesis (unpublished), Kyushu University, Japan. 318pp.

Sikumbang, N. and Heryanto, R., 2009. *Geological map of the Banjarmasin Quadrangle, Kalimantan. Scale 1:250,000*. Geological Research and Development Centre of Indonesia. Bandung.

Sukamto, R., 1982. *Geological map of Pangkajene and western part of Watampone Quadrangles, Sulawesi. Scale 1:250,000*. Geological Research and Development Centre of Indonesia. Bandung.

Wakita, K., Munasri., Sopaheluwakan, J., Zulkarnain, I., and Miyazaki, K., 1994a. Early Cretaceous tectonic events implied in the time-lag between the age of radiolarian chert and its metamorphic basement in the Bantimala area, South Sulawesi, Indonesia. *The Island Arc*, 3, p.90-102.

Wakita, K., Munasri. and Bambang, W., 1994b. Cretaceous radiolarians from the Luk Ulo Complex in the Karangsambung area, central Java, Indonesia. *Journal of SE Asian Earth Sciences*, 9, p.29-43.

Wakita, K., Sopaheluwakan, J., Miyazaki, K., Zulkarnain, I., and Munasri., 1996. Tectonic evolution of the Bantimala Complex, South Sulawesi, Indonesia, *In*: Hall, R., Blundell, D.J. (Eds.), Tectonic Evolution of Southeast Asia. *Geological Society of London Special Publication*, 106, p.353-364.

Wakita, K., Miyazaki, K., Zulkarnain, I., Sopaheluwakan, J., and Sanyoto, P., 1998. Tectonic implications of new age data for the Meratus Complex of south Kalimantan, Indonesia. *The Island Arc*, 7, p.202-222.

Whitney, D.L. and Evans, B.W., 2010. Abbreviations for names of rock-forming minerals. *American Mineralogist,* 95, p.185-187.

Williams, P.R., Johnston, C.R., Almond, R.A., and Simamora, W.H., 1988. Late Cretaceous to Early Tertiary structural elements of West Kalimantan. *Tectonophysics*, 178, p.279-297.

Wilson, M.E.J. and Moss, S.J., 1999. Cenozoic palaeogeographic evolution of Sulawesi and Borneo. *Palaeogegraphy, Palaeoclimotology, Palaeoecology*, 145, p.303-337.

Yuwono, Y.S., Priyomarsono, S., Maury, R.C., Rampnoux, J.P., Soeria-Atmadja, R., Bellon, H., and Chotin, P., 1988. Petrology of the Cretaceous magmatic rocks from Meratus Range, southeast Kalimantan. *Journal of Southeast Asian Earth Sciences*, 2, p.15-22.

Zulkarnain, I., 2003. Quartz-Chloritoid rock from Bobaris Range South Kalimantan, Indonesia. *RISET - Geologi dan Pertambangan*, 13, p.27-38.